Focus Article

Peptide and protein-based nanotubes for nanobiotechnology

Anna Petrov and Gerald F. Audette*

The development of biologically relevant nanosystems such as biomolecular probes and sensors requires systems that effectively interface specific biochemical environments with abiotic architectures. The most widely studied nanomaterial, carbon nanotubes, has proven challenging in their adaptation for biomedical applications despite their numerous advantageous physical and electrochemical properties. On the other hand, development of bionanosystems through adaptation of existing biological systems has several advantages including their adaptability through modern recombinant DNA strategies. Indeed, the use of peptides, proteins and protein assemblies as nanotubes, scaffolds, and nanowires has shown much promise as a bottom-up approach to the development of novel bionanosystems. We highlight several unique peptide and protein systems that generate protein nanotubes (PNTs) that are being explored for the development of biosensors, probes, bionanowires, and drug delivery systems.

How to cite this article:
WIREs Nanomed Nanobiotechnol 2012, 4:575–585. doi: 10.1002/wnan.1180

INTRODUCTION

The rapidly evolving field of nanotechnology presents constant demands on the scientific community to advance and create new materials to be used in medicine (diagnostics, drug delivery, and tissue engineering), electronics (memory storage, nanoelectronics, quantum computers, novel semiconductor, and optoelectronic devices), bioseparation, catalysis etc. The most studied nanomaterial is carbon nanotubes (CNTs), which possess highly desirable properties including excellent tensile strength, large surface area, favorable electronic, thermal and chemical characteristics.[1] It is these properties that make CNTs interesting vehicles for a variety of areas such as delivery of genes and drugs into bodies, biosensors, and as scaffolds for engineered tissues. However, there are numerous concerns about the toxicity and biodegradability of CNTs,[1–4] adverse effects to electrical properties[5] as a result of exposure to humidity, oxygen, N_2O, and NH_3, as well the lack of solubility in aqueous solutions present significant challenges for the use of CNTs in biological and/or biomedical applications.

One approach to mitigating the challenges of CNT solubility and cytotoxicity is to modify the CNTs with biomolecules. For instance, some groups have modified CNTs with chitosan derivatives or incorporated them into a chitosan matrix[6,7] or coated CNTs with proteins[8–10] to improve biocompatibility for tissue engineering.[3,4] While these approaches show distinct promise, a separate approach is to make the nanotubes entirely of peptides or proteins. Protein-based nanotubes can be particularly desirable for biomedical applications due to, for example, assembly under physiologically-relevant conditions as well as their ease of functionalization through protein engineering approaches. We focus on several interesting peptide and protein nanotube (PNT) systems that are showing promise as nanotubes for biomedical applications.

PEPTIDE NANOTUBES

Peptides, being much shorter than their protein counterparts, often lack the secondary and tertiary structures (i.e., α-helices, β-sheets) associated with proteins. This general lack of initial secondary structure makes peptides an interesting choice for nanotube development, primarily through the induction of secondary structure upon nanotube formation. Indeed,

*Correspondence to: audette@yorku.ca
Department of Chemistry and Centre for Research on Biomolecular Interactions, York University, Toronto, Ontario, Canada

there has been significant interest in developing peptide nanotubes for various applications,[11,12] and several examples of stable nanotubes have been built from simple peptides, ranging from 0.7 to 1000 nm in diameter with varying rigidities. For instance in 2008, Valéry and colleagues[13] reported that the small (eight-residue) synthetic peptide lanreotide self-assembled into amyloid-like nanotubes in water. While examining the role of the β-hairpin conformation of the peptide and aromatic residues in lanreotide, the authors established that the three aromatic side chains of the peptide did not have equivalent roles in self-assembly. Indeed, the naphthalene and tyrosine side chains were found to be responsible for peptide–peptide interactions, while the tryptophan, part of the β-hairpin conformation in lanreotide, was found to be responsible for the lateral filament stacking.[13] Other groups have also demonstrated the assembly of nanostructures from a variety of peptide modalities including fluorescently labeled dipeptides,[14] tripeptides,[15] and tetrapeptides,[16,17] as well as modified cyclic peptides[18] and peptide-poly(ethylene glycol) conjugates.[19] The architectures and stabilities of these nanostructures are generated in part through the hydrogen bonding patterns and induced secondary structure, often β-sheet, inherent in the peptide precursors.

The assembly of peptide nanotubes under facile conditions suggests that they may be adapted as scaffolds for biologically based nanowires. Indeed, Reches and Gazit[20] demonstrated the potential for creation of a peptide-based nanowire. In this study, the authors found that a Phe–Phe dipeptide from an amyloidogenic hexapeptide provided the necessary attractive forces to generate stable micrometer-length nanotubes. The peptide nanotubes provided an internal pore that could be filled with an ionic silver solution; the peptide could then be removed through digestion with proteinase K, resulting in a bare silver nanowire.[20] These data demonstrate that the peptide nanotube could be used as a casting mould for metal nanowires, as well as a biological encasement for the same nanowires, depending on whether the peptide is digested away or not. Further studies into these peptide nanotubes has shown that these peptide precursors can assemble into different nanostructures depending on the treatment of the peptide prior to initiation of oligomerization,[21,22] and that they exhibit significant piezoelectricity[23] and photoluminescence.[24,25] The development of biomedical devices incorporating these peptide nanotube based devices shows distinct promise, either on their own or as casting moulds for metal nanowires.

PROTEIN NANOTUBES

The increased complexity inherent in fully folded proteins, that is their native tertiary structure, presents an interesting challenge in the development of these systems as nanotubes. The question of how does one use a protein's native structure to assemble into a nanotube, either via a patterned template or through self-assembly is of central importance in developing a PNT. Because of the inherent challenges associated with *de novo* design of PNTs from fully folded proteins, several groups have undertaken an adaptation bacterial flagella and pili, the fiber-like protein polymers produced by many bacteria for a variety of functions. Outlined below are several examples of flagella and pilin-based PNTs, as well as several other protein-based PNTs.

Flagella-Based PNTs

Flagella, fiber-like structures produced by bacteria for cellular motility, are structurally composed of three general multi-protein components: a proton gradient-driven motor complex, a joint structure, and long helical fiber. Native flagella are 10–15 μm in length with inner and outer diameters of 2–3 nm and 12–25 nm, respectively;[26] the helical fiber is generated from thousands of copies of the FliC (flagelin) protein. In 2006, Kumara et al. reported the self-assembly of a flagellin-based PNT using a FliC-thioredoxin fusion protein, denoted FliTrx.[27] The FliTrx construct fused 109 thioredoxin residues between Gly-243 and Ala-352 of FliC such that the thioredoxin active site was readily accessible by several loop peptides designed to be presented on the PNT surface. FliTrx PNTs were observed through fluorescence microscopy to form 4–10 μm bundles (Figure 1). The authors subsequently reported a layer-by-layer assembly of streptavidin-FliTrx and polyethylenimine-FliTrx PNTs for a more uniform assembly of these PNTs on surfaces,[28] and the utilization of FliTrx-based PNTs as a scaffold for the synthesis of metal (Ag, Au, Cd, Co, Cu, and Pd) nanoparticles and nanotubes under mildly reducing conditions[29] (Figure 1). The FliTrx monomer was modified to include a series of peptide loops separated in the quaternary structure of the PNT to facilitate an ordered metal binding on the PNT surface, suggesting the utilization of these FliTrx-based PNTs in sensing and nanoelectronics applications.[29]

The flagellin subunit FliC has also been utilized as a potential vector for liposome-based drug delivery. In particular Ngweniform et al. assembled FliC-based PNTs, which display an overall anionic surface, for coordination of cationic liposomes.[30] The authors

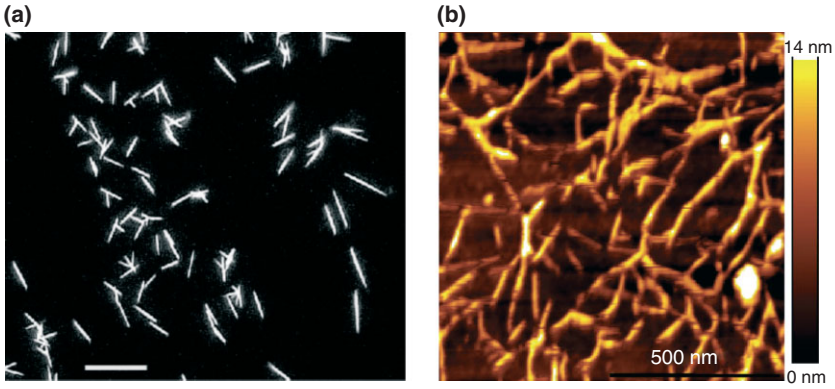

FIGURE 1 | Flagella-based PNTs. (a) Fluorescent microscopic image of self-assembled FliTrx PNTs (scale bar = 10 μm).[27] The recombinant FliTrx construct can be readily modified to contain a variety of surface accessible loops for tailored binding of a variety of molecules, in this case the dye NanoOrange (Reprinted with permission from Ref 27. Copyright 2006 American Chemical Society). (b) Atomic force microscopy image of mineralized FliTrx PNTs. Thirteen PNTs were generated in a layer-by-layer method separating layers of FliTrx protein containing an engineered glutamate-aspartate (negatively charged) surface-exposed peptide loop with layers of calcium carbonate (Ca_2CO_3).[28] The assembly process can be used to assemble FliTrx PNTs with a variety of metals (i.e., Ag, Au, Cd, Co, Cu, and Pd) nanoparticles. (Reprinted with permission from Ref 28. Copyright 2007 American Chemical Society).

demonstrated that FliC-based PNTs are able to coordinate zinc phthalocyanine (ZnPC), a model photodynamic anti-cancer therapeutic, enclosed in cationic liposomes.[30] Coordination of the ZnPC liposomes by the FliC-PNTs resulted in a increase in liposome stability through a reduction in ZnPC vibrational motion. It has been suggested that this increase in liposome stability through PNT coordination will result in longer circulation times, and the ability to genetically modify the FliC protein prior to PNT assembly should facilitate targeted delivery of the PNT-coordinated drug-loaded liposomes.[30]

Pilin-Based PNTs

Type IV Pili (T4P) are flexible hair-like structures produced at the poles of many gram-negative bacteria. Native T4P are 6 nm in diameter and have a length of up to several micrometers, which the bacteria can control by retraction and extension of pili via a complex type II secretion system,[31–33] and are involved in a range of processes. For instance, the opportunistic pathogen *Pseudomonas aeruginosa* utilizes T4P to initiate cellular infection through interaction with specific cellular glycolipids,[34–40] provide motility,[31,32,41–43] facilitate DNA uptake,[44,45] biofilm formation,[46,47] and are used to adhere to abiotic surfaces.[48,49] T4P have been shown to be robust structures, withstanding shear forces of over 100 pN per T4P[50,51] and extension/retraction rates of ~0.5 μm/seconds.[32,40] T4P are polymers of a single monomeric type IV pilin (PilA) subunit, a protein comprised of a four-stranded antiparallel β-sheet wrapped around one end of a long α-helix[33,52–55] (Figure 2). A C-terminal disulfide-bound loop region is the receptor-binding domain (RBD) that mediates interactions with cellular receptors and abiotic surfaces,[48,49,52–55] while the N-terminal portion of the α-helix is utilized as an hydrophobic oligomerization domain in native T4P.[37,38,52–55] Removal of the exposed N-terminal region of the α-helix results in a highly soluble pilin monomer that retains the antigenic and receptor-binding characteristics of the native protein.[52–55] It was this engineered pilin monomer that was observed to assemble into PNTs that are similar in morphology and diameter (~6 nm) to native T4P (Figure 2); PNT assembly is triggered in the presence of hydrophobic compounds.[56]

Preassembled pilin-based PNTs have been observed to bind to stainless steel in a manner similar to the binding observed for T4P,[48,49] an interaction mediated by the tip-associated RBD. The attractive force between the RBD or PNT and steel is in the range of 26–55 pN and 78–165 pN, respectively.[48,49] These values, which would represent three RBDs per PNT tip, are similar to, albeit slightly less than, the attractive forces observed for native T4P.[45,60] These data suggest that the pilin-based PNT:surface interaction is reasonably robust. In addition, pilin-based PNTs can be assembled from surface constrained hydrophobes, a useful characteristic for the development of PNT-based nanoelectronics. Based on an initial study of PNT assembly from hydrophobes constrained to a microtiter plate,[56] pilin-based PNT oligomerization was subsequently observed from self-assembled monolayers (SAMs)

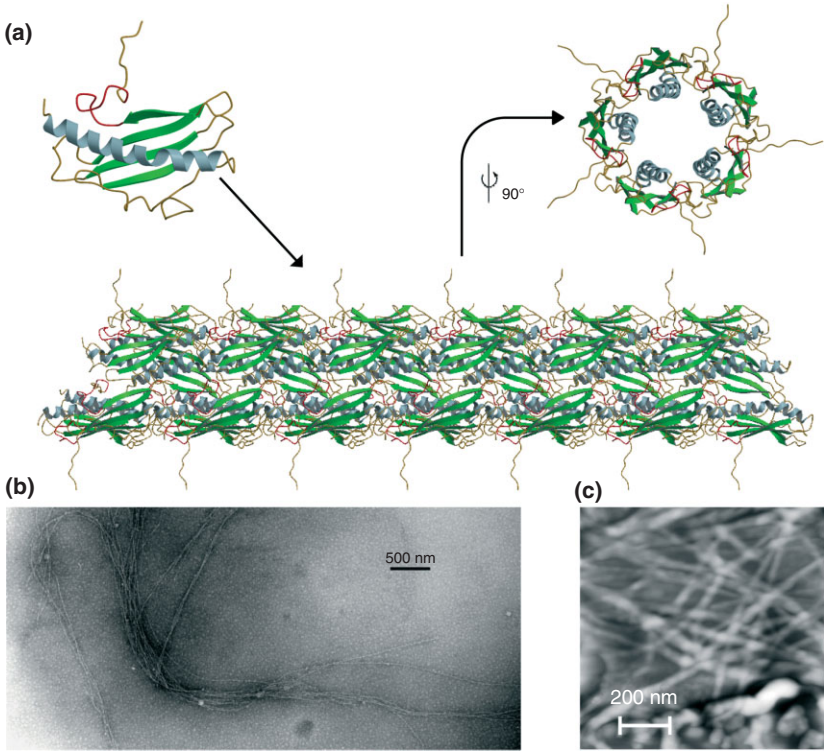

FIGURE 2 | Pilin-derived PNTs. (a) The structure of the monomeric K122-4 pilin (PDB ID 1QVE),[54] and model of the K122-4 pilin-derived PNTs. The N-terminal α-helix is in light blue, the β-sheet is in green, coil regions in gold, and the receptor-binding domain, known to mediate surface interactions,[48,49,52–55] is in red. PNTs assemble in the presence of a hydrophobic compound,[56,57] via a multi-start helix[38,56] into PNTs with predicted inner and outer diameters of 2 and 6 nm, respectively.[56] (b) Transmission electron microscope image of solution-oligomerized pilin-derived PNTs. PNTs exhibit similar morphology and antigenic characteristics, although they are longer, as native T4P.[34] (c) Atomic force microscopy image of pilin-derived PNTs from a self-assembled alkylthiol monolayer on a Au(III) surface. The surface-tethered assembly of the pilin-derived PNTs presents opportunities for the use of pilin-derived PNTs multiple nano-applications such as biosensors, biowires, etc. Panel (a) was produced using Molscript[58] and Raster3D;[59] (panel (b): Reprinted with permission from Ref 56. Copyright 2004 American Chemical Society; panel (c) Reprinted with permission from Ref 57. Copyright 2009 American Scientific Publishers).

of alkylthiols on Au(111) surfaces[57] (Figure 2(c)). Coupling these observations with the knowledge that pilin-derived PNTs can bind DNA[45,56] and the high sequence variation of the pilins[33,45,56] suggests that the pilin-based PNTs may be useful in a variety of nanotechnology applications including biosensing, bioseparations, and bionanoelectronics.

In addition to PNTs generated from engineered pilin monomers, functional nanostructures have been generated from native bacterial pili. While not technically nanotubes as the native pilus is itself a nanofiber, these structures are indeed interesting and show distinct promise for application development. For instance, the type IV pili of *Geobacter sulfurreducens* were shown to mediate the reduction of Fe(III) oxides,[61] suggesting that the pili are acting as biological nanowires with potential applications in microbial-based fuel cells etc. Indeed, further studies have demonstrated that the *G. sulfurreducens* pili-based system works very well in microbial fuel cells.[62] Furthermore, these pili-based nanowires have been shown to have long-range metallic-like conductivity[63] and to impart supercapacitor behavior[64] when used in the context of *G. sulfurreducens* biofilm-based microbial fuel cells, both important aspects for energy storage applications. Also, a very recent report of Cao and colleagues demonstrates that a native type I pili isolated from *E. coli* organized into three-dimensional lattices.[65] The isolated pili were also found to be amenable to the formation of silica-pili hybrids with various nanoassemblies,[65] implicating these structures for use in a range of applications.

OTHER PROTEIN NANOTUBES

Self-Assembled PNTs

There are several examples of self-assembled PNTs generated from non-pilin or flagellar proteins. For instance, Ballister and colleagues reported PNT self-assembly from Hcp1, a 17.4 kDa protein of the

P. aeruginosa type IV secretion system.[66] Hcp1-derived PNTs adopt a hexameric ring structure with lengths of up to 100 nm (~25 4.4 nm high subunit rings), an outer diameter of 9.0 nm, a height of 4.4 nm, and an inner cavity of 4.0 nm. The Hcp1 protein rings in the PNT stack non-helically and are held together by mechanical compatibility and engineered disulfide-bonding through G90S and R157S mutations. An intriguing aspect of this study in the ability to control PNT length through introduction of chain-terminating subunits, as well as the capability to distinguish PNT polarity by incorporation of uniquely engineered protein caps.[66] Another example of a non-pilin PNT is the recently reported PNTs generated from the Trp RNA-binding attenuation protein (TRAP) from the thermophilic bacteria *Bacillus stearothermophilus*.[67] TRAP monomers form 11-mer rings that polymerize into PNTs of approximately 8 nm in diameter.[67] A third example of a non-pilin PNT is the observed self-assembly of the milk protein α-lactalbumin,[68] where a partial proteolytic hydrolysis acts as a trigger for self-assembly. PNTs derived from α-lactalbumin appear to be 10-start helical right-handed structures with outer and inner diameters of 20 and 8.7 nm, respectively. Mass spectral analysis indicated that PNT subunits were composed of a mixture of products from proteolysis of the α-lactalbumin precursor.[68] While this result may affect PNT homogeneity, it does demonstrate the potential for proteolytic triggering of PNT generation from a precursor protein, for example, a fusion protein.

When discussing self-assembling protein systems, one must also mention amyloids and amyloid-like fibrils. The self-assembly of amyloid and amyloid-like fibrils has been an area of significant research over the past several years, particularly in the context of neurodegenerative disorders such as Alzheimer's and prion-associated diseases. There are numerous excellent reviews on the structure and assembly of amyloid fibrils,[69–77] to which the interested reader is directed. Amyloid self-assembly is based primarily on β-strand complimentarily that enables protein aggregation into fibril structures;[73,76] the resultant fibril is exceedingly stable and can adopt large-scale structures, in addition to the known disease-related amyloid plaques.[69] With respect to their usage in biomaterials and nanotechnology, amyloids have been proposed to be used as protein scaffolds,[69,73] nanowires,[71] in organic solar cells,[78] based in large part on their inherent fibril structure.[73]

Template-Assembled PNTs

An alternative to using self-assembling proteins for PNT generation is to use a template-assisted assembly, which can provide a means of patterned PNT assembly followed by removal of the template layer resulting in free PNTs. In recent study, Tao and colleagues[79] employed a layer-by-layer approach to prepare PNTs composed of two proteins, bovine serum albumin (BSA), and lyophilized hemoglobin from bovine erythrocytes, from glutaraldehyde (GA)-functionalized alumina membranes. The use of the alumina template allowed for uniform PNT length, while pore size and PNT outer diameters could be tailored based upon the alumina support or number of layering steps, respectively. The authors suggested that these template-generated PNTs could be further functionalized, with enzymes or antibodies, to perform targeted catalytic or recognition functions.[79]

In another layer-by-layer assembly, human serum albumin (HSA) PNTs were generated by alternating layers of HSA with poly-L-arginine (PLA) from an etched polycarbonate membrane based on the difference in overall net charge between HSA (negative) and PLA (positive).[80] The resultant HSA/PLA nanotubes were of uniform length, with an outer diameter and wall thickness of 417 $\pm$ 16 and 56 $\pm$ 7 nm, respectively, and were able to bind magnetite (Fe_3O_4) on their outer surface enabling the magnetic capture of the Fe_3O_4-HSA/PLA nanotubes. Interestingly, the HSAs within the PNT architecture were able to bind zinc(II)-protoporphyrin IX (ZnPP), an analog of the iron(III)-protoporphyrin (hemin) that is released by methemoglobin in the circulatory system.[80] The authors suggest that the magnetic capture of Fe_3O_4-HSA/PLA nanotubes present an promising avenue for bioseparation, the efficient nanoscale separation, and recovery of biomolecules from complex mixtures, and an important component of any nanomedical regiment.

The development of PNT-based biocatalysts has also been explored using layer-by-layer methodologies; the inclusion of an enzyme into the PNT architecture (in whole or in part) provides a specific biocatalytic function. One such example of a biocatalytic PNT is that of the layer-by-layer assembly of cytochrome-C PNTs[81] with either GA or poly-(sodium styrenesulfonate). The cytochrome-C within the PNT architecture retained its native tertiary structure and catalytic activity, suggesting usage of these PNTs in cytochrome-C-specific biocatalytic reactions.[81] Another example of template assembly of catalytic PNTs is that of Hou and colleagues.[82] In this study, the authors generated glucose oxidase (GOx) and hemoglobin (Hb) PNTs with alternating layers of protein and GA. In both instances the enzymatic PNTs retained either glucose oxidation or heme electroactivity.[82] In a separate study,

Komatsu and colleagues reprised their HSA/PLA nanotubes, but coated the inner surface with catalytically active GOx.[83] Finally, Yang et al. generated gold-nanoparticle (Au NP) containing lysozyme PNTs in an aim to generate bionanowires.[84] A lysozyme-Au NP mixture spontaneously formed hollow, branched Au NP-embedded PNTs following incubation under ambient conditions for 7 days. While PNTs were not directly demonstrated to function as nanowires, they were shown to be stable at 100 W sonication (30 min), or under incubation with 1M HCl or 1M NaOH (overnight);[84] such stability may prove highly beneficial for development of these hybrid PNTs for nanomedical applications.

Virus-Based Nanotubes

Another approach to developing PNTs for nanotechnological/nanomedical applications is the adaptation of viral coat proteins. Many viruses are conveniently rod shaped and their capsids self-assemble from relatively simple protein building blocks,[85,86] which makes them good raw material for nanotube development. For instance, the rod-shaped tobacco mosaic virus (TMV) normally self-assembles in a helical fashion to enclose its RNA genome;[87] however, it has been shown to generate nanodisks and nanotubes under selective conditions.[86,88] Miller et al.,[88] using a recombinant TMV coat protein for chormophore attachment, demonstrated that with simple adjustments of pH and ionic strength, nanodisks and rods with lengths of over 100 nm could be generated (Figure 3). While minimal energy transfer was observed between monomers, nanodisks exhibited a better energy transfer, with marked improvement upon assembly into rods. The resulting TMV nanorods exhibited efficient (>90 %) light transfer over a broad set of wavelengths.[88] TMV-based nanowires have also been generated through a sensitization/electroless deposition strategy.[89,90] In these studies, purified, empty TMV particles were initially sensitized with Pd(II) followed by an electroless deposition of either copper[89] or zinc[90] to the inner and outer TMV surface, respectively. Metal deposition was in the form of nanoparticles at the protein surface, each with an appropriate observed energy profile for the deposited nanoparticles.[89,90] The use of modified TMV particles is therefore envisioned to play a role in nanosystems such as nanoscale optical devices and/or nanodevice wiring.

A second tubular nanostucture generated from viral capsid proteins is that of the cowpea chlorotic mottle virus (CCMV).[86] In this study, a DNA scaffold was employed to helically assemble PNTs of various lengths (from less than 200 nm to over a micron) with a 17 nm diameter from the 20 kDa CCMV coat protein. Control of PNT length was achieved through the ratio of DNA length to protein concentration; the largest PNTs (>5 μm) were observed in reactions where 5–10 DNA base pairs were available per protein dimer.[86] The authors suggest that metal deposition into these PNTs may be achievable,[86] which is analogous to metalized TMV-based PNTs discussed above.

Another virus that has been explored for the development of protein-based bionanowires is the M13 bacteriophage. This process is again a two-step procedure in which the protein scaffold, in this case modified M13 phage coat protein(s), is first assembled and then a conducting molecule selectively aggregates onto the PNT scaffold. A plasmid-driven expression of recombinant M13 coat proteins pIII and pVIII was shown to facilitate the synthesis of gold nanowires; the gold-binding recombinant pIII and pVII proteins were identified through a biopanning process.[91] The resultant M13-scaffolded Au-nanoparticles were wire-like

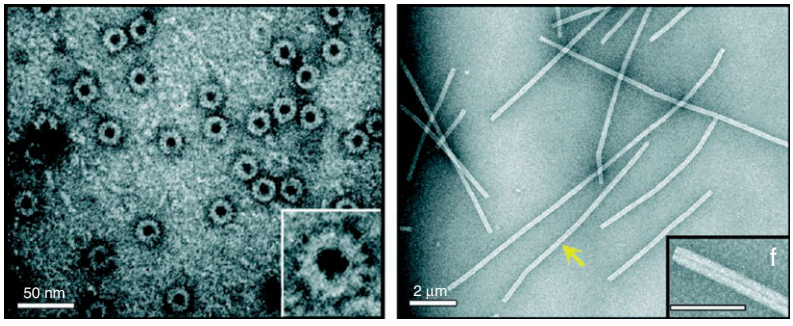

FIGURE 3 | Viral-based nanodisks and nanotubes. Transmission electron microscopy images of chromophore-containing nanodisks (left) and nanotubes (right) generated from synthesized from modified TMV coat protein.[88] Scale bars represent 50 nm (left panel), 200 nm (right panel), and 100 nm (panel inset 'f'). TMV nanodisks are layered heptadecameric structures. A single 900-nm-long TMV PNT (yellow arrow; right panel) contains over 6300 choromphore molecules.[88] (Reprinted with permission from Ref 88. Copyright 2007 American Chemical Society)

structures of 10 nm in width and ~1 μm in length, and continuous nanowires of ~40 nm diameter were achieved after ~5 min of electroless deposit. Electrical transport characterizations of the M13-scaffolded Au-nanowires showed reproducible continuous current and calculated resistance of about 1.8×10^{-6} Ωm, about 100 times higher resistance than bulk gold.[91] In a similar study, Nam et al. genetically modified the pVIII coat protein to express four consecutive N-terminal glutamates to serve as a template to produce Co_3O_4 nanowires[92] (Figure 4). Cobalt oxide was found to uniformly mineralize along the length of the tube, and alteration of the Co solution could produce nanowires of differing morphologies. Introduction of an Au-binding peptide motif into the pVIII protein enabled the researchers to create a pVIII-Au-Co_3O_4 hybrid bionanowire (Figure 4). When compared to the pure cobalt oxide wires, the pVIII-Au-Co_3O_4 hybrid bionanowire was observed to generate higher (~30%) initial and reversible storage capacity,[92] suggesting the utility of these nanocomposites in applications from batteries to medical implants. Recent studies on the use of modified M13-phage nanowires demonstrate promising electrochemical properties for microbatteries,[93,94] both as M13-Co oxide nanowires[93] and as M13-$FePO_4$ bound to CNTs as a nanocomposite cathode material.[94] In this later study, the pVIII protein of the M13 viral coat was bound $FePO_4$ while the pIII protein facilitated interaction with single-walled carbon nanotubes (SWCNTs) thereby bridging the biologically ordered nanowires with the desirable electronic characteristics of the CNTs within the cathode material;[94] the electrochemical profiles of these M13-based microbatteries were favorable compared to capacities based on crystalline $LiFePO_4$ batteries.[94] These studies show distinct promise for developing biologically based nanosources of power for biomedical applications, for example, implantable biosensors.

CONCLUSION

Given the richness of diversity in structures, biocompatibility, and adaptability through genetic engineering, peptide and protein-based nanotubes present unique alternatives to CNT scaffolds for new nanomedical and bionanotechnological applications. The in-built assembly characteristics of flagella, pili, and viral coat proteins are examples of self-assembling nanosystems that show distinct promise in the design and development of bionanosystems for nanomedicine, drug delivery, bionanowiring, etc. In addition, template-assisted PNT generation of layered

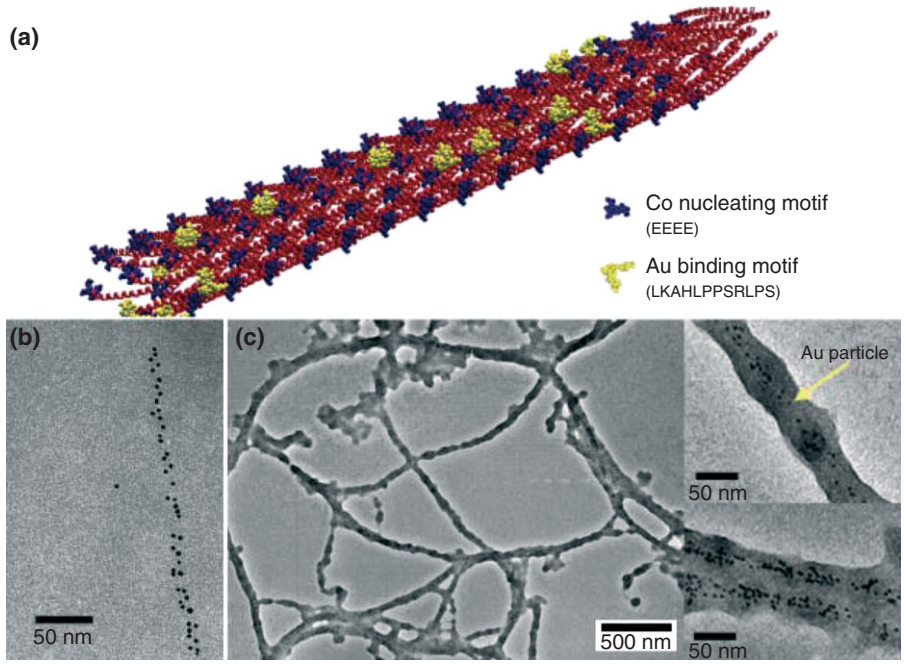

FIGURE 4 | Virus-based bionanowires. (a) Schematic representation of engineered M13 phage pVIII coat protein (red) PNTs containing Co (blue) and Au (yellow) binding motifs. (b) Transmission electron microscope (TEM) image of gold nanoparticles assembled by the Au-binding domains of pVIII-derived PNTs. (c) TEM images Au/Co_3O_4 nanowires assembled from pVIII-PNTs derived from protein expressed in the presence of Co_3O_4. The assembled nanowires were shown to generate higher (~30%) initial and reversible storage capacity than pure Co_3O_4 wires.[92] (Reprinted with permission from Ref 92. Copyright 2006 American Association for the Advancement of Science)

PNTs presents opportunities to develop multifunctional PNTs that may be targeted to a specific cellular location through surface-exposed epitopes. Understanding of not only the functional characteristics of these nanosystems, but also their modes of assembly, kinetics, and stabilities will provide a greater understanding of the molecular requirements of these systems for inclusion in targeted bionanocomposites. These developments will lead to new bionano approaches to the treatment of disease as well as novel implantable devices such as bio-based computing, molecular wires, and integrated biosensors.

ACKNOWLEDGMENTS

This work was supported by grants from the Natural Sciences & Engineering Council of Canada (NSERC), the Canadian Foundation for Innovation, and York University (to GFA). AP acknowledges financial support from the Ontario Graduate Scholarship Program and York University.

REFERENCES

1. Smart SK, Cassady AI, Lu GQ, Martin DJ. The biocompatibility of carbon nanotubes. *Carbon* 2006, 44:1034–1047.
2. Aillon KL, Xie Y, El-Gendy N, Berkland CJ, Forrest ML. Effects of nanomaterial physicochemical properties on *in vivo* toxicity. *Adv Drug Deliv Rev* 2009, 61:457–466.
3. Li X, Fan Y, Watari F. Current investigations into carbon nanotubes for biomedical application. *Biomed Mater* 2010, 5:22001.
4. Li X, Gao H, Uo M, Sato Y, Akasaka T, Feng Q, Cui F, Lui X, Watari F. Effect of carbon nanotubes on cellular functions *in vitro*. *J Biomed Mater Res A* 2009, 91:132–129.
5. Fatouros DG, Power K, Kadir O, Dékány I, Yannopoulos SN, Bouropoulos N, Bakandritsos A, Antonijevic MD, Zouganelis GD, Roldo M. Stabilisation of SWNTs by alkyl-aulfate chitosan derivatives of different molecular weight: towards the preparation of hybrids with anticoagulant properties. *Nanoscale* 2011, 3:1218–1224.
6. Carson L, Kelly-Brown C, Stewart M, Oki A, Regisford G, Luo Z, Bakhmutov VI. Synthesis and characterization of chitosan-carbon nanotube composites. *Mater Lett* 2009, 63:617–620.
7. Dieckmann GR, Dalton AB, Johnson PA, Razal J, Chen J, Giordano GM, Muñoz E, Musselman IN, Baughman RH, Draper R. Controlled assembly of carbon nanotubes by designed amphiphilic peptide helices. *J Am Chem Soc* 2003, 125:1770–1777.
8. Shen J-W, Wu T, Want Q, Kang Y. Induced stepwise conformational change of human serum albumin. *Biomaterials* 2008, 29:3847–3855.
9. Ge C, Du J, Zhao L, Wang L, Liu Y, Li D, Yang Y, Zhou R, Zhao Y, Chai Z, et al. Binding of blood proteins to carbon nanotubes reduces cytotoxicity. *Proc Natl Acad Sci U S A* 2011, 108:16968–16973.
10. Griggoryan G, Kim YH, Acharya R, Axelrod K, Jain RM, Willis L, Drndic M, Kikkawa JM, DeGrado WF. Computational design of virus-like protein assemblies on carbon nanotube surfaces. *Science* 2011, 332:1071–1076.
11. Gao X, Matsui H. Peptide-based nanotubes and their applications in bionanotechnology. *Adv Mater* 2005, 17:2037–2050.
12. Scanlon S, Aggeli A. Self-assembling peptide nanotubes. *Nano Today* 2008, 3:22–30.
13. Valéry C, Pouget E, Pandit A, Verbavatz J-M, Bordes L, Boisdé I, Cherif-Cheikh R, Artzner F, Paternostre M. Molecular origin of the self-assembly of lanreotide into nanotubes: a mutational approach. *Biophysical J* 2008, 94: 1782–1795.
14. Tang C, Smith AM, Collins RF, Uljin RV, Saiani A. Fmoc-diphenylalanine self-assembly mechanism induces apparent pK_a shifts. *Langmuir* 2009, 25:9447–9453.
15. Xu H, Das AK, Horie M, Shaik MS, Smith AM, Luo Y, Lu X, Collins R, Liem SY, Song A, et al. An investigation of the conductivity of peptide nanotube networks prepared by enzyme-triggered self-assembly. *Nanoscale* 2010, 2:960–966.
16. Stone DA, Hsu L, Stupp SI. Self-assembling quinquethiphene-oligopeptide hydrogelators. *Soft Matter* 2009, 5:1990–1993.
17. Sun Y, Jiang L, Schuermann KC, Adrieaens W, Zhang L, Boey FYC, De Cola L, Brunsveld L, Chen X. Semiconductive, one-dimensional, self-assembled nanostructures based on oligopeptides with π-conjugated segments. *Chem Eur J* 2011, 17:4746–4749.
18. Ashkenasy N, Horne WS, Ghadiri MR. Design of self-assembling peptide nanotubes with delocalized electronic states. *Small* 2006, 2:99–102.
19. Schillinger E-K, Mena-Osteritz E, Hentschel J, Börner HG, Bäuerle P. Oligothipphene versus β-sheet peptide: synthesis and self-assembly of an organic semiconductor-peptide hybrid. *Adv Mater* 2009, 21:1562–1567.

20. Reches M, Gazit E. Casting metal nanowires within discrete self-assembled peptide nanotubes. *Science* 2003, 300:625–627.
21. Amdursky N, Molotskii N, Gazit E, Rosenman G. Elementary building blocks of self-assembled peptide nanotubes. *J Am Chem Soc* 2010, 132:15632–15636.
22. Amdursky N, Beker P, Koren I, Bank-Srour B, Mishina E, Semin S, Rasing T, Rosenberg Y, Barkay Z, Gazit E, et al. Structural transition in peptide nanotubes. *Biomacromolecules* 2011, 12:1349–1354.
23. Kholkin A, Amdursky N, Bdikin I, Gazit E, Rosenman G. Strong piezoelectricity in bioinspired peptide nanotubes. *ACS Nano* 2010, 4:610–614.
24. Amdursky N, Molotskii M, Aronov D, Adler-Abramovich L, Gazit E, Rosenman G. Blue luminescence based on quantum confinement at peptide nanotubes. *Nano Lett* 2009, 9:3111–3115.
25. Amdursky N, Koren I, Gazit E, Rosenman G. Adjustable photoluminescence of peptide nanotube coatings. *J Nanosci Nanotechnol* 2011, 11:9282–9286.
26. Yonekura K, Maki-Yonekura S, Namba K. Complete atomic model of the bacterial flagellar filament by electron cryomicroscopy. *Nature* 2003, 424:643–650.
27. Kumara MT, Srividya N, Muralidharan S, Tripp BC. Bioengineered flagella protein nanotubes with cysteine loops: self-assembly and manipulation in an optical trap. *Nano Lett* 2006, 6:2121–2129.
28. Kumara MT, Tripp BC, Muralidharan S. Layer-by-layer assembly of bioengineered flagella protein nanotubes. *Biomacromolecules* 2007, 8:3718–3722.
29. Kumara MT, Tripp B, Muralidharan S. Self-assembly of metal nanoparticles and nanotubes on bioengineered flagella Scaffolds. *Chem Mater* 2007, 19:2056–2064.
30. Ngweniform P, Li D, Mao C. Self-assembly of drug-loaded liposomes on genetically engineered protein nanotubes: a potential anti-cancer drug delivery vector. *Soft Matter* 2009, 5:954–956.
31. Strom MS, Lory S. Structure-function and biogenesis of the type IV pili. *Annu Rev Microbiol* 1993, 47:565–596.
32. Mattick JS. Type IV pilli and twitching motility. *Annu Rev Microbiol* 2002, 56:289–31.
33. Shala A, Ferraro M, Audette GF. Bacterial secretion systems: nanomachines for infection and genetic diversity. In: Bawa R, Audette GF, Rubenstein I, eds. *Clinical Nanomedicine: From Bench to Bedside*. Singapore: Pan Sanford Publishing; 2012, 1–19. In press.
34. Audette GF, Hazes B. Development of protein nanotubes from a multi-purpose biological structure. *J Nanosci Nanotech* 2007, 7:2222–2229.
35. Folkhard W, Marvin DA, Watts TH, Paranchych W. Structure of polar pili from *Pseudomonas aeruginosa* strains K and O. *J Mol Biol* 1981, 149:79–93.
36. Hahn HP. The type-4 pilus is the major virulence-associated adhesin of *Pseudomonas aeruginosa*—a review. *Gene* 1997, 192:99–108.
37. Marvin DA, Nadassy K, Welsh LC, Forest KT. Type-4 bacterial pili: molecular models and their simulated diffraction patterns. *Fibre Diffraction Rev* 2003, 11:87–94.
38. Craig L, Pique ME, Tainer JA. Type IV pilus structure and bacterial pathogenicity. *Nat Rev Microbiol* 2004, 2:363–378.
39. Burrows LL. Weapons of mass retraction. *Mol Microbiol* 2008, 57:878–888.
40. Hansen JK, Forest KT. Type IV pilin structures: insights on shared architectures, fiber assembly, receptor binding and type II secretion. *J Mol Microbiol Biotechnol* 2006, 11:192–207.
41. Skerker JM, Berg HC. Direct observation of extension and retraction of type IV pili. *Proc Natl Acad Sci U S A* 2001, 98:6901–6904.
42. Conrad JC, Gibiansky ML, Jin F, Gordon VD, Motto DA, Mathewson MA, Stopka WG, Zelasko DC, Shrout JD, Wong GC, et al. Flagella and pili-mediated near-surface single-cell motility mechanisms in *P. aeruginosa*. *Biophys J* 2011, 100:1608–1616.
43. Jin F, Conrad JC, Gibiansky ML, Wong GC. Bacterial use type-IV pili to slingshot on surfaces. *Proc Natl Acad Sci U S A* 2011, 108:12617–12622.
44. Dubnau D. DNA uptake in bacteria. *Annu Rev Microbiol* 1999, 53:217–244.
45. Van Schaik EJ, Giltner CL, Audette GF, Keizer DW, Slupsky CM, Sykes BD, Irvin RT. DNA binding: a novel function of *Pseudomonas aeruginosa* Type IV Pili. *J Bacteriol* 2005, 187:1455–1464.
46. Barken KB, Pamp SJ, Yang L, Gjermansen M, Bertrand JJ, Klausen M, Givskov M, Whitchurch CB, Engel JN, Tolker-Neilsen T. Roles of type IV pili, flagellum-mediated motility and extracellular DNA in the formation of mature multicellular structures in *Pseudomonas aeruginosa* bioflims. *Environ Microbiol* 2008, 10:2331–2343.
47. Mikkelsen H, Sivaneson M, Filloux A. Key two-component regulatory systems that control biofilm formation in *Pseudomonas aeruginosa*. *Environ. Microbiol* 2011, 13:1666–1681.
48. Giltner CL, van Schaik EJ, Audette GF, Kao D, Hodges RS, Hassett DJ, Irvin RT. The *Pseudomonas aeruginosa* type IV pilin receptor binding domain functions as an adhesin for both biotic and abiotic surfaces. *Mol Microbiol* 2006, 59:1083–1096.
49. Yu B, Giltner CL, van Schaik EJ, Bautista DL, Hodges RS, Audette GF, Li DY, Irvin RT. A novel biometallic interface: high affinity tip-associated binding by pilin-derived protein nanotubes. *J Bionanosci* 2007, 1:1–11.

50. Maier B, Potter L, So M, Long CD, Seifert HS, Sheetz MP. Single pilus motor forces exceed 100 pN. *Proc Natl Acad Sci U S A* 2002, 99:16012–16017.
51. Merz AJ, So M, Sheetz MP. Pilus retraction powers bacterial twitching motility. *Nature* 2000, 407:98–102.
52. Hazes B, Sastry PA, Hayakawa K, Read RJ, Irvin RT. Crystal structure of *Pseudomonas aeruginosa* PAK pilin suggests a main-chain-dominated mode of receptor binding. *J Mol Biol* 2000, 299:1005–1017.
53. Keizer DW, Slupsky CM, Kalisiak M, Campbell AP, Crump MP, Sastry PA, Hazes B, Irvin RT, Sykes BD. Structure of a pilin monomer from *Pseudomonas aeruginosa*. *J Biol Chem* 2001, 276:24186–24193.
54. Audette GF, Irvin RT, Hazes B. Crystallographic analysis of the *Pseudomonas aeruginosa* strain K122-4 monomeric pilin reveals a conserved receptor binding architecture. *Biochemistry* 2004, 43:11427–11435.
55. Kao DJ, Churchill ME, Irvin RT, Hodges RS. Animal protection and structural studies of a consensus sequence vaccine targeting the receptor binding domain of the type IV pilus of *Pseudomonas aeruginosa*. *J Mol Biol* 2007, 374:426–442.
56. Audette GF, van Schaik EJ, Hazes B, Irvin RT. DNA-binding protein nanotubes: learning from nature's nanotech examples. *Nano Lett* 2004, 4:1897–1902.
57. Lombardo S, Zahedi-Jasbi S, Jeung S-K, Morin S, Audette GF. Initial studies of protein nanotube oligomerization from a modified gold surface. *J Bionanosci* 2009, 3:61–65.
58. Kraulis J. MOLSCRIPT: a program to produce both detailed and schematic plots of protein structures. *J Appl Cryst* 1991, 24:946–950.
59. Merritt EA, Bacon DJ. Raster3D photorealistic molecular graphics. *Methods Enzymol* 1997, 277:505–524.
60. Touhami A, Jericho MH, Boyd JM, Beveridge TJ. Nanoscale characterization and determination of adhesion forces of *Pseudomonas aeruginosa* pili by using atomic force microscopy. *J Bacteriol* 2006, 188:370–377.
61. Reguera G, McCarthy KD, Mehta T, Nicoll JS, Tuominen MT, Lovely DR. Extracellular electron transfer via microbial nanowires. *Nature* 2005, 423:1098–1101.
62. Yi H, Nevin KP, Kim B-C, Franks AE, Klimes A, Tender LM, Lovley DR. Selection of a variant of *Geobacter sulfurreducens* with enhanced capacity for current production in microbial fuel cells. *Biosens Bioelectron* 2009, 24:3498–3503.
63. Malvankar NS, Vargas M, Nevin KP, Franks AE, Leang C, Kim B-C, Inoue K, Mester T, Covalla SF, Johnson JP, et al. Tunable metallic-like conductivity in microbial nanowire networks. *Nat Nanotechnol* 2011, 6:c573–c579.
64. Malvankar NS, Metser T, Tuominen MT, Lovley DR. Supercapacitors based on c-type cytochromes using conductive nanostructured networks of living bacteria. *ChemPhysChem* 2012, 13:463–468.
65. Cao B, Xu H, Mao C. Controlled self-assembly of rod-like bacterial pili particles into ordered lattices. *Angew Chem Int Ed* 2011, 50:6264–6268.
66. Ballister ER, Lai AH, Zuckermann RN, Cheng Y, Mougous JD. *In vitro* self-assembly of tailorable nanotubes from a simple protein building block. *Proc Natl Acad Sci U S A* 2008, 105:3733–3738.
67. Miranda FF, Iwasaki K, Akashi S, Sumitomo K, Kobayashi M, Yamashita I, Tame JRH, Heddle JG. A Self-Assembled Protein Nanotube with High Aspect Ratio. *Small* 2009, 5:2077–2084.
68. Graveland-Bikker JF, Koning RI, Koerten HK, Geels RBJ, Heeren RMA, de Kruif CG. Structural characterization of α-lactalbumin nanotubes. *Soft Matter* 2009, 5:2020–2026.
69. Lu K, Jacob J, Thiyagarajan P, Conticello VP, Lynn DG. Exploiting amyloid fibril lamination for nanotube self-assembly. *J Am Chem Soc* 2003, 125:6391–6393.
70. Paparcone R, Cranford SW, Buehler MJ. Self-folding and aggregation of amyloid nanofibrils. *Nanoscale* 2011, 3:1748–1755.
71. Scheibel T, Parthasarathy R, Sawicki G, Lin X-M, Jaeger H. Conducting nanowires built by controlled self-assembly of amyloid fibers and selective metal deposition. *Proc Natl Acad Sci U S A* 2003, 100:4527–4532.
72. Greenwald J, Reik R. Biology of amyloid: structure, function and regulation. *Structure* 2010, 18:1244–1260.
73. Knowles TPJ, Buehler MJ. Nanomechanics of functional and pathological amyloid materials. *Nat Nanotechnol* 2011, 6:469–479.
74. Pederson JS, Anderson CB, Otzen DE. Amyloid structure - one but not the same: the many levels of fibrillar polymorphism. *FEBS J* 2010, 277:4591–4601.
75. Toyama BH, Weissman JS. Amyloid structure: conformational diversity and consequences. *Annu Rev Biochem* 2011, 80:577–585.
76. Colby W, Prusiner SB. Prions. *Cold Spring Harb Perspect Biol* 2011, 3:a006833.
77. Zerovnik E, Stoka V, Mirtic A, Guncar G, Grdadolnik J, Stainforth RA, Turk D, Turk V. Mechanisms of amyloid fibril formation - focus on domain-swapping. *FEBS J* 2011, 278:2263–2282.
78. Barrau S, Zhang F, Herland A, Mammo W, Andersson MR, Inanas O. Integration of amyloid nanowires in organic solar cells. *Appl Phys Lett* 2008, 93:023307.
79. Tao C, Yang S, Zhang J. Template-synthesized protein nanotubes with controlled size based on layer-by-layer method. *Chin J Chem* 2010, 28:325–328.
80. Komatsu T, Kobayashi N. Protein nanotubes bearing a magnetite surface exterior. *Polym Adv Technol* 2010, 22:1315–1318.

81. Tian Y, He Q, Cui Y, Li J. Fabrication of protein nanotubes based on layer-by-layer assembly. *Biomacromolecules* 2006, 7:2539–2542.

82. Hou S, Wang J, Martin CR. Template-synthesized protein nanotubes. *Nano Lett* 2005.5:231–234.

83. Komatsu T, Terada H, Kobayashi N. Protein nanotubes with an enzyme interior surface. *Chem Eur J* 2010, 17:1849–1854.

84. Yang T, Zhang Y, Li Z. Formation of gold nanoparticle decorated lysozyme microtubes. *Biomacromolecules* 2011, 12:2027–2031.

85. Mao C, Solis D, Reiss BD, Kottmann ST, Sweeney RY, Hayhurst A, Georgiou G, Iverson B, Belcher AM. Virus-based toolkit for the directed synthesis of magnetic and semiconducting nanowires. *Science* 2004, 303:213–217.

86. Mukherjee S, Pfeifer CM, Johnson JM, Liu J, Zlotnik A. Redirecting the coat protein of a spherical virus to assemble into tubular nanostructures. *J Am Chem Soc* 2006, 128:2538–2539.

87. Klug A. The tobacco mosaic virus particle: structure and assembly. *Phil Trans R Soc Lond B* 1999, 354:531–535.

88. Miller RA, Presley AD, Francis MB. Self-assembling light-harvesting systems from synthetically modified tobacco mosaic virus coat proteins. *J Am Chem Soc* 2007, 129:3104–3109.

89. Balci S, Bittner AM, Hahn K, Scheu C, Knez M, Kadri A, Wege C, Jeske H, Kern K. Copper nanowires within the central channel of tobacco mosaic virus. *Electrochimica Acta* 2006, 51:6251–6257.

90. Balci S, Bittner AM, Schirra M, Thonke K, Sauer R, Hahn K, Kadri A, Wege C, Jaske H, Kern K. Catalytic coating of virus particles with zinc oxide. *Electrochimica Acta* 2009, 54:5149–5154.

91. Huang Y, Chiang C-Y, Lee SK, Gao Y, Hu EL, Yoreo JD, Belcher AM. Programmable assembly of nanoarchitectures using genetically engineered viruses. *Nano Lett* 2005, 5:1429–1434.

92. Nam KT, Kim D-W, Yoo PJ, Chiang C-Y, Meethong N, Hammond PT, Chiang Y-M, Belcher AM. Virus-enabled synthesis and assembly of nanowires for lithium ion battery electrodes. *Science* 2006, 312:885–888.

93. Nam KT, Wartena R, Yoo PJ, Liau FW, Lee YJ, Chiang Y-M, Hammond PT, Belcher AM. Stamped microbattery electrodes based on self-assembled M13 viruses. *Proc Natl Acad Sci U S A* 2008, 105:17227–17231.

94. Lee YJ, Yi H, Kim W-J, Kang K, Yun DS, Strano MS, Ceder G, Belcher AM. Fabricating genetically engineered high-power lithium-ion batteries using multiple virus genes. *Science* 2009, 324:1051–1055.

